Nickelalumite, ideally NiAl4(SO4)(OH)12(H2O)3 , a new-old mineral from the Kara-Tangi uranium deposit, Kyrgyzstan

Vladimir Yu. Karpenko
  Russian Academy of Sciences

Atali A. Agakhanov
  Russian Academy of Sciences

Leonid A. Pautov
  Russian Academy of Sciences

Galiya K. Bekenova
  Satpaev Institute of Geological Sciences

Yulia A. Uvarova
  CSIRO Mineral Resources, ARRC

Elena Sokolova
  University of Manitoba

Tamara V. Dikaya
  Russian Academy of Sciences

Frank C. Hawthorne (✉ frank.hawthorne@umanitoba.ca)
  University of Manitoba

Research Article

Additional Declarations: No competing interests reported.

Abstract

Nickelalumite, ideally $NiAl_4(SO_4)(OH)_{12}(H_2O)_3$, is a newly approved mineral from the Batken region, Kyrgyzstan, where it occurs in the Kara-Tangi and Kara-Chagyr uranium deposits. It is found in the zone of hydrothermal alteration of U−V-bearing carbon-rich silicified schists, in association with quartz, calcite, alumohydrocalcite, allophane, crandallite, kyrgyzstanite, ankinovichite and an unknown Al−OH-mineral. Nickelalumite formed by hydrothermal alteration of U−V bearing carbon-rich silicified schists. It occurs as aggregates of colourless to pistachio-green radiating bladed crystals from 0.05 to 0.50 mm long. It is vitreous to transparent in thin flakes, has a white streak, and shows no fluorescence under long-wave or short-wave ultraviolet light. Cleavage is perfect parallel to {001} and no parting was observed. Mohs hardness is 2, it is brittle and has a splintery fracture. The calculated density is 2.231 g.cm^{-3}. In transmitted plane-polarized white light, nickelalumite is non-pleochroic, biaxial, α = 1.542(2), γ = 1.533(2), β could not be measured due to the almost negligible thickness of the flakes. Electron-microprobe analysis gave Al_2O_3 39.94, SiO_2 0.17, SO_2 12.16, V_2O_3 0.29, FeO 0.15, NiO 8.00, ZnO 6.21, $(H_2O)_{calc}$. 31.87, sum 98.79 wt%, H_2O was determined by crystal-structure analysis, and the empirical formula is as follows: $(Ni_{0.55}Zn_{0.39}V_{0.02}Fe_{0.01})_{\Sigma0.97}(Al_{3.99}Si_{0.01})_{\Sigma4.00}(SO_4)(OH)_{12}(H_2O)_3$ based on 4 (Al + Si) cations. There is considerable variation in substitution of Zn, Cu and Fe for Ni and V for S. The crystal structure of nickelalumite was refined to an R_1 index of 5.66% and consists of interrupted $[NiAl_4(OH)_{12}]$ sheets intercalated with layers of $\{(SO_4)_2(H_2O)_3\}$; nickelalumite is a member of the chalcoalumite group.

Introduction

Nickelalumite, $(Ni_{0.55}Cu_{0.25})_{\Sigma1.00}Al_4[SO_4]_{\Sigma0.75}(NO_3)_{\Sigma0.50}(OH)_{12}(H_2O)_3$, was first described from the Mbobo Mkulu cave, Nelspruit district, eastern Transvaal, together with two other minerals: mbobomkulite, $(Ni,Cu^{2+})Al_4[(NO_3),(SO_4)]_2(OH)_{12}(H_2O)_3$, and hydrombobomkulite, $(Ni,Cu^{2+})Al_4[(NO_3),(SO_4)]_2(OH)_{12}(H_2O)_{12}$ (Martini 1980). Mbobomkulite and hydrombobomkulite were approved by IMA-CNMMN but nickelalumite was rejected because of some problems with chemical composition (J. Martini, pers. comm.). Nickelalumite was stated to be the nickel analogue of chalcoalumite, $CuAl_4(SO_4)(OH)_{12}(H_2O)_3$, a 17.090 Å, b 8.915 Å, c 10.221 Å, β 95.88°, sp.gr. $P2_1$ (Larsen and Vassar 1925; Williams and Khin 1971).

During investigation of vanadium-bearing schists from Kyrgyzstan, we found nickelalumite as a constituent of crystalline crusts at Kara-Chagyr and Kara-Tangi (Karpenko 2004a). The nickelalumite crystals at the Kara-Tangi are of reasonable quality and allowed the structure of the mineral to be refined (Uvarova et al. 2005) and properties to be measured accurately. Thus we chose Kara-Tangi as the type locality for nickelalumite which has been approved as a new mineral species by the IMA-CNMNC, 2022-071. Dr. Martini declined to participate in the IMA approval procedure, stating that he is now out of mineralogy; however, he welcomed our initiative to formalize the mineral. Here we describe nickelalumite from all three localities. The holotype sample from Kara-Tangi is deposited in the systematic collection (# 98105) at the A.E. Fersman Museum, Moscow, Russia.

Occurrence

In the southern part of the Fergana valley, a belt of outcrops of black carbon-rich schists extends for 100 km along the foothills of the Alai range. The schists are part of the South Fergana mélange involving large blocks of Early Paleozoic carbon-rich siliceous rocks in a matrix of serpentinite. Initially investigated by Scherbakov (1924), Preobrazhensky (1926) and many others, the schists contain extensive U-Ni-Zn-V mineralization. The most significant exposures are at Kara-Tangi and Kara-Chagyr in the Batken region, Kyrgyzstan (Karpenko et al. 2004a) and show extensive Ni-Zn-V mineralization (Agakhanov et al. 2005; Karpenko et al. 2004a, b; 2009; 2011; 2016), and nickelalumite was found at both these localities. At Kara-Tangi, there is a minor U-deposit that was worked in the 1960−1970s (V. Rogovoy, pers. comm.) and is located in a gorge (Fig. 1a) with the same name on the northern slope of the Katran-Tau mountains, Batken region, Kyrgyzstan. The deposit occurs in a zone of strongly folded chlorite-sericite slates (Fig. 1b) of Upper-Silurian age, and the mineralization occurs in boudinaged carboniferous black schists. The size of the lenses ranges from one metre to several tens of metres in length.

Nickelalumite was found in the dumps of the mine adit on the right side of Kara-Tangi gorge. It forms pale-blue to greenish crusts of radiating lamellar aggregates of crystals up to 1.5 mm on the surface of carbon-rich siliceous schist in the dump from the adit, and in cracks and small cavities (Fig. 2) associated with quartz, calcite, alumohydrocalcite, kyrgyzstanite, ankinovichite and boehmite. Some aggregates are replaced by allophane. Nickelalumite crystals are lamellar and split (Figs. 3a,b), and resemble kyrgyzstanite, the zincian analogue of nickelalumite (Agakhanov et al. 2005).

At Kara-Chagyr, nickelalumite occurs as crusts of radiating fibrous aggregates up to 1.5 mm which are commonly intercalated with allophane and are closely associated with ankinovichite, Zn-Ni-bearing volborthite, allophane, tyuyamunite and rare tangeite (Fig. 4a). In cavities in the rock, it can form almost ideal spheres up to 1.5 mm in diameter growing on lamellar skeletal crystals of volborthite (Fig. 4b). Here, nickelalumite shows complex zoning (Figs. 4c,d), and for this reason, nickelalumite from Kara-Tangi was chosen as the holotype material.

Physical properties

Nickelalumite occurs as aggregates of radiating bladed crystals from 0.05 to 0.50 mm long (Fig. 4); individual crystals disaggregate into fibres and flakes that deform under the slightest touch. Colour varies from almost colourless through light blue to pistachio green depending on crystal size and V content. Nickelalumite is vitreous to transparent in thin crystals, has a white streak, and shows no fluorescence under long-wave or short-wave ultraviolet light. Cleavage is perfect parallel to {001} and no parting was observed. Mohs hardness is 2, it is brittle and has a splintery fracture. The calculated density is 2.231 g.cm^{-3} and it is soluble in hot (1:1) HCl.

In transmitted plane-polarized white light, nickelalumite is non-pleochroic. A spindle stage was used to orient a crystal for measurement of refractive indices in white light (Bartelmehs et al. 1992). Nickelalumite is biaxial, α = 1.542(2), γ = 1.533(2), β could not be measured due to the almost negligible thickness of

the flakes. Extinction is oblique (~ 40°). The average refractive index for vanadium-bearing nickelalumite (V_2O_5 6. % wt.) from Kara-Chagyr is ~ 1.575–1.580, in accord with the refractive indices of ankinovichite, the vanadium analogue of nickelalumite (Karpenko et al. 2004a, b).

Raman Spectroscopy

The Raman spectrum of nickelalumite from Kara-Tangi (Fig. 5a) was obtained at room temperature on a polished crystal using a Thermo DXR2xi Raman imaging confocal microscope with a green laser (532 nm). The output power of the laser beam was 8 mW (at 80% power), the holographic diffraction grating had 400 lines cm^{-1}, spectral resolution was 2 cm^{-1}, and data were collected from 50 to 6000 cm^{-1}. The diameter of the focal spot on the sample was 2 μm. The backscattered Raman signal was collected with a 100x objective; signal-acquisition time for a single scan of the spectral range was 0.3 s and the signal was averaged over 30 scans. The spectrum was processed using Omnic software. Two sharp lines at 3674 and 3614 cm^{-1} correspond to (OH)-stretching. There are two distinct (OH) groups in the structure: (1) those where the donor O bonds to two [6]Al, and (2) those where the donor O bonds to two [6]Al plus [6]Zn. The latter will have stronger hydrogen bonding and hence will occur at lower stretching frequency: 3614 cm^{-1}. There is a broad absorption in the range 2800–3500 cm^{-1} that corresponds to (H_2O) stretching. An intense band at 987 cm^{-1} and a weak band at 1108 cm^{-1} correspond to the v_1 and v_3 symmetric stretching of the (SO_4) tetrahedra; the band at 604 cm^{-1} corresponds to bending vibrations of (SO_4); and the weak band at 468 cm^{-1} is associated with (SO_4) and (AlO_6) bending modes.

A similar spectrum was obtained from tiny flakes of nickelalumite (sample #MGS 18211) obtained from the National Museum of Natural History, Pretoria, Republic of South Africa, courtesy of D. Bernardo, Council for Geoscience, South Africa (Fig. 5b).

Chemical Composition

In order to understand why nickelalumite was not approved originally by IMA-CNMMN, we examined powder sample #MGS 18211 in BSE mode. It consists of thin plates of pure nickelalumite mixed with Al–Si-rich material, probably allophane (Martini 1980), that resulted in excess Si in the formula.

The original analysis of nickelalumite from Mbobo Mkulu, South Africa (Martini 1980) (analysis 1, Table 1) included 4.70 wt% N_2O_5 and a deficiency in S (0.75 *apfu*), suggesting replacement of $(SO_4)^{2-}$ by $(NO_3)^{2-}$. In this regard, Williams et al. (2011) reported the synthesis of $NiAl_4(NO_3)_2(OH)_{12}(H_2O)_x$ with highly disordered interlayer $(NO_3)^-$ oxyanions. They dehydrated their disordered material to $[ZnAl_4(OH)_{12}](NO_3)_2$ and showed that the structure contains $[ZnAl_4(OH)_{12}]$ layers topologically the same as those in nickelalumite, supporting the idea that $(NO_3)^{2-}$ may replace $(SO_4)^{2-}$ in the nickelalumite structure.

Table 1
Chemical composition (wt%) for nickelalumite (1−4) and kyrgyzstanite (5)

Components	1	2	3	4	5
Al_2O_3	39.3	41.65	39.94	38.99−40.63	38.45
V_2O_3	–	–	0.29	0.11−0.40	0.06
SiO_2	8.95	–	0.17	0.11−0.23	0.33
SO_3	10.28	13.53	15.2	14.82−15.56	15.00
NiO	6.59	10.08	8.00	7.54−8.62	4.13
ZnO	n.g.	not det	6.21	5.73−6.88	10.02
CuO	2.35	0.93	n.d.		0.58
FeO	–	–	0.15	0.04−0.25	0.32
N_2O_5	4.70	–	n.d.		0.00
C	< 0.30	–	n.d.		n.d.
H_2O	28.53	–	31.87		30.10
Sum	100.7		98.79		99.01

1, 2: Mbobo Mkuku, R.S.A. (Martini 1980) (1: blue nodules in allophane, wet chemistry; 2: crust on gypsum, microprobe); 3, 4: nickelalumite, used for crystal refinement, Kara-Tangi, Kyrgyzstan, our data (3: average from 10 microprobe analysis; 4: range of composition); 5: kyrgyzstanite, Kara-Tangi, Kyrgyzstan, average from 6 microprobe analysis (Agakhanov et al. 2005)

Empirical formulae:

1: $(Ni_{0.55}Cu_{0.25})_{\Sigma1.00}Al_4[SO_4]_{\Sigma0.75}(NO_3)_{\Sigma0.50}(OH)_{12}(H_2O)_3$ (Martini 1980)

2: $(Ni_{0.55}Zn_{0.39}V_{0.02}Fe_{0.01})_{\Sigma0.97}(Al_{3.99}Si_{0.01})_{\Sigma4.00}(SO_4)(OH)_{12}(H_2O)_3$ (calculated on (Al + Si) = 4 cations)

3: $(Ni_{0.55}Zn_{0.39}V_{0.02}Fe_{0.01})_{\Sigma0.97}(Al_{3.99}Si_{0.01})_{\Sigma4.00}(SO_4)(OH)_{12}(H_2O)$ (Agakhanov et al. 2005)

The composition of nickelalumite was obtained for the crystal used for X-ray diffraction. It was mounted on a Perspex disc, ground, polished, carbon-coated and analyzed with a Cameca SX 100 electron microprobe operating in wavelength-dispersion mode with an accelerating voltage of 15 keV, a specimen current of 3 nA, a beam size of 20 microns and counting times on peak and background of 20 and 10 s, respectively. The following standards and crystals were used for K X-ray lines: Al: andalusite; Si: titanite; S: anhydrite; V: VP_2O_7 ; Ni: Ni_2Si ; Zn: gahnite; Fe: fayalite; Cu: $CuFeS_2$. Data were reduced using the $\Phi(\rho z)$ procedure (Merlet 1992). The amount of H_2O was derived from structure refinement. Table 1 gives the chemical composition and empirical formula unit based on 4 (Al + Si) cations: $(Ni_{0.55}Zn_{0.39}V_{0.02}Fe_{0.01})_{\Sigma0.97}(Al_{3.99}Si_{0.01})_{\Sigma4.00}[SO_4](OH)_{12}(H_2O)_3$. The composition of kyrgyzstanite, a Zn-analogue of nickelalumite, is given for comparison (analysis 5, Table 1).

Variation in chemical composition of nickelalumite at both Kara-Tangi and Kara-Chagyr was examined with Jeol Superprobe 733 and JXA-50A electron microprobes equipped with Link energy-dispersive spectrometers. The experimental conditions were as follows: for the Jeol Superprobe 733: accelerating voltage 20 kV, specimen current 1 x 10^{-9} A, standards: Al_2O_3 (Al), ZnS (S), magnetite USNM (Fe), metallic V and Cu (V, Cu), NiO (Ni), quartz (Si); for the JXA-50A microprobe: accelerating voltage 20 kV, specimen current 3 x 10^{-9} A; standards: microcline USNM 143966 (Si, Al), ilmenite USNM 96189 (Fe), gahnite USNM 145883 (Zn), metallic V and Cu (V, Cu), NiO (Ni), barite (S). Following ZAF corrections, formulae were calculated based on 6 (Ni + Zn + Cu + Fe + V + Al + Si + S) apfu and are given in Table 2.

Table 2
Chemical composition for nickelalumite (representative local microprobe analyses, wt%)

Component	1	2	3	4	5	6	7	8	9	10	11	12	13	14
Al_2O_3	39.24	39.54	37.36	38.59	37.76	37.67	37.73	38.83	38.05	36.35	38.99	38.77	38.01	39.02
V_2O_3	0.40	0.52	0.78	0.68	0.00	0.17	0.09	0.00	0.00	4.42	4.59	4.15	8.06	7.18
SiO_2	0.15	0.00	0.00	0.00	0.38	0.41	0.64	0.69	0.77	1.08	0.61	1.10	3.79	1.33
SO_3	15.71	16.07	15.67	16.18	14.38	14.11	14.54	14.80	14.45	11.99	13.10	11.96	9.46	11.83
NiO	9.06	11.01	11.50	10.45	7.05	9.87	8.08	10.03	12.07	10.03	8.87	7.77	10.81	9.90
ZnO	5.12	3.86	3.50	3.93	6.64	4.88	6.24	4.83	0.66	1.15	0.34	2.25	2.86	1.46
CuO	0.00	0.00	0.00	0.00	0.72	0.10	0.52	0.22	0.00	1.10	0.31	0.95	2.21	1.92
FeO	0.00	0.00	0.00	0.00	0.00	0.29	0.33	0.00	0.00	0.00	0.00	1.80	0.00	0.42
Total	69.68	71.00	68.81	69.83	66.93	67.50	68.17	69.40	66.00	66.12	66.81	68.75	75.20	73.06
Formula calculated on 6 (Ni + Zn + Cu + Fe + V + Al + Si + S) *apfu*														
Ni^{+2}	0.63	0.75	0.81	0.73	0.51	0.71	0.57	0.70	0.87	0.73	0.63	0.54	0.71	0.67
Zn^{+2}	0.33	0.24	0.23	0.25	0.44	0.32	0.41	0.31	0.04	0.08	0.02	0.14	0.17	0.09
Cu^{+2}	0.00	0.00	0.00	0.00	0.05	0.01	0.03	0.01	0.00	0.08	0.02	0.06	0.14	0.12
Fe^{+2}	0.00	0.00	0.00	0.00	0.00	0.02	0.02	0.00	0.00	0.82	0.00	0.13	0.00	0.03
V^{+3}	0.03	0.04	0.05	0.05	0.00	0.01	0.01	0.00	0.00	0.32	0.33	0.29	0.43	0.40
Al^{+3}	3.99	3.95	3.87	3.93	4.00	3.95	3.93	3.96	4.03	3.88	4.07	3.96	3.65	3.85
Si^{+4}	0.01	0.00	0.00	0.00	0.03	0.04	0.06	0.06	0.07	0.10	0.05	0.10	0.31	0.11
S^{+6}	1.02	1.02	1.03	1.05	0.97	0.94	0.96	0.96	0.98	0.82	0.87	0.78	0.58	0.74

1–8: nickelalumite, Kara-Tangi (light-blue radiate-fibrous segregations); 9–14: nickelalumite, Kara-Chagyr (9: light-blue needle-shaped, 10–12: light-green spherulites of V-bearing nickelalumite; 13, 14: dark-green spherulites of high-vanadium nickelalumite); 1–4, 13, 14: microprobe analysis, our data; 5–12: Karpenko et al. 2004a

Variation in Ni content is linear with (Zn + Cu + Fe) content (Fig. 6a). The data for Kara-Tangi fall almost exactly along the line (Ni + Zn + Cu + Fe) = 1 *apfu* and show isomorphism between Ni and Zn, which leads to the nickelalumite–kyrgyzstanite series. The data for Kara- Chagyr are slightly displaced below the line, suggesting that there is an additional element at the Ni site in Kara-Tangi nickelalumite. In the interlayer, V shows an inverse linear correlation with S (Fig. 6b), primarily in the Kara-Chagyr samples, and there is a positive correlation between the intensity of (green) colour and the V content. It is possible that incorporation of some V^{3+} could also occur at the Ni site *via* the substitution $(VO_4)^{3-} + V^{3+} \rightarrow (SO_4)^{2-} + Ni^{2+}$ which would account for the displacement of most of the Kara-Chagyr samples below the line in Fig. 6a. Karpenko et al. (2004) suggested the substitution $(SO_4)^{2-} + Al^{3+} \leftrightarrow (VO_4)^{3-} + Si^{4+}$, which leads to V–Si-bearing nickelalumite (analyses 13 and 14, Table 2). The complexity of the compositional variations involving (Ni, Zn), Al, V and S in nickelalumite–ankinovichite is apparent on the characteristic X-ray maps of those elements (Fig. 7).

X-ray Powder Diffraction

X-ray powder diffraction data for nickelalumite were collected on a 57.3 mm RKD powder camera using Ni-filtered Cu$K\alpha$ X-radiation and the data are listed in Table 3. Unit-cell parameters refined from powder data are as follows: $a = 10.219(10)$, $b = 8.863(12)$, $c = 17.103(15)$ A, $\beta = 95.25(10)°$, $V = 1543(2)$ Å^3, $Z = 4$.

Table 3
X-ray powder-diffraction pattern for nickelalumite

I	d_{obs} (Å)	d_{calc} (Å)	h k l
10	8.35	8.515	0 0 2
3	6.67	6.684	1 1 0
3	4.62	4.556	2 0 – 2
9	4.27	4.258	0 0 4
2	3.71	3.693	1 1 – 4
5	3.30	3.317	2 2 – 1
4	3.16	3.177, 3.179	2 2 – 2, 0 1 5
6	3.02	3.049	2 2 2
6	2.683	2.701	0 2 5
2	2.592	2.598	2 1 5
8	2.508	2.501, 2.510	4 0 – 2, 2 3 1
7	2.276	2.291, 2.278	2 3 3, 4 0 – 4
3	2.222	2.216	0 4 0
2	2.067	2.065	1 1 – 8
9	1.981	1.987	4 0 – 6
3	1.824	1.823	5 2 1
3	1.811	1.814	4 0 6
4	1.740	1.740	1 2 – 9
4	1.710	1.712	4 0 – 8
1	1.647	1.653	4 1 7
3	1.556	1.555	2 3 – 9
6	1.480	1.476	6 3 – 1
6	1.455	1.456, 1.456	6 3 1, 0 6 2
4	1.400	1.397	6 3 3
4	1.361	1.359	4 0 10
1	1.302	1.306, 1.298	6 3 – 7, 2 3 11
1	1.272	1.272, 1.272	8 0 0, 4 6 – 2
1	1.241	1.239, 1.242	4 6 – 4, 8 0 2
1	1.217	1.216	0 0 14
4	1.189	1.189, 1.188	8 0 4, 2 3 – 13

a = 10.219(10) b = 8.863(12) c = 17.103(15) β = 95.26(10) V = 1543(2)

Single-crystal X-ray Data Collection And Refinement

X-ray diffraction data for nickelalumite were collected with a Bruker $P4$ diffractometer equipped with a 4K CCD detector (Mo$K\alpha$ radiation) from a single-crystal of nickelalumite with dimensions 0.10 x 0.06 x 0.02 mm. The intensities of 7103 reflections with $-10 < h < 10$, $-9 < k < 9$, $-18 < l < 18$ were collected to 59.99° 2θ using 30 s per 0.2° frame: an empirical absorption correction (SADABS, Sheldrick 2008) was applied. The refined unit-cell parameters were obtained from 3365 reflections with $I > 20\sigma I$. There were no data in the region between 59.99° and 45°, and the data were truncated to 44.42°. The crystal structure of nickelalumite was solved using the Patterson method and refined to $R_1 = 0.057$ and a GoF value of 1.059 for 1554 independent reflections (281 refined parameters including extinction) with the Bruker SHELXTL version 5.1 system of programs. Site occupancy was refined for the M site (occupied primarily by Ni and Zn, plus minor V and Fe).

Details of the data collection and structure refinement are given in Table 4, final atom parameters are given in Table 5, selected interatomic distances and angles in Table 6, details of hydrogen bonding in Table 7, and refined site-scattering values and assigned populations for selected sites are given in Table 8.

Further details of data collection and structure refinement can be retrieved from the Crystallographic Information File (CIF) included in Supplementary Information.

Table 4
Miscellaneous refinement data for nickelalumite

a (Å)	10.2567(5)
b	8.8815(4)
c	17.0989(8)
β	95.548(1)
V (Å^3)	1550.3(2)
Space group	$P2_1/n$
Z	4
Absorption coefficient (mm^{-1})	1.71
F(000)	1064.0
$D_{calc.}$ (g.cm^{-3})	2.231
Crystal size (mm)	0.10 x 0.06 x 0.02
Radiation/ filter	MoKα/graphite
2θ-range for data collection (°)	44.42
R(int) (%)	2.82
Reflections collected	26624
Unique reflections	15173
Independent reflections	1959
$F_o > 4\sigma F_o$	1554
Refinement method	Full-matrix least squares on F^2, fixed weights proportional to 1/σ F_o^2
Goodness of fit on F^2	1.059
Final $R_{(obs)}$ (%) [$F_o > 4\sigma F_o$]	$R1$ = 5.66
R indices (all data) (%)	$R1$ = 7.04
	$wR2$ = 16.72
	Goo$F$ = 1.054

Table 5
Final atom positions and displacement parameters (Å) for nickelalumite

	x	y	z	U_{eq}*	U_{11}	U_{22}	U_{33}	U_{23}	U_{13}	U_{12}
M	0.74867(8)	0.49993(8)	0.49280(5)	0.0068(4)	0.0026(6)	0.0023(7)	0.0157(7)	−0.0003(3)	0.0017(4)	−0.0001(3)
$Al(1)$	0.0001(2)	0.3286(2)	0.5016(1)	0.0081(6)	0.0061(13)	0.0053(13)	0.0128(13)	−0.0002(8)	0.0004(10)	−0.0001(8)
$Al(2)$	0.5005(2)	0.6741(2)	0.5045(1)	0.0083(6)	0.0055(13)	0.0054(13)	0.0140(13)	−0.0004(8)	0.0006(10)	0.0003(8)
$Al(3)$	0.2485(2)	0.1611(2)	0.4976(1)	0.0076(6)	0.0059(12)	0.0032(13)	0.0136(13)	−0.0001(8)	0.0014(10)	0.0002(8)
$Al(4)$	0.2496(2)	−0.1606(2)	0.5001(1)	0.0075(6)	0.0057(12)	0.0024(13)	0.0143(13)	−0.0004(8)	0.0007(10)	−0.0004(8)
O(1)	0.5816(5)	0.4971(4)	0.5540(3)	0.0066(12)	0.0052(25)	0.0054(27)	0.0092(26)	−0.0020(18)	0.0003(20)	0.0016(18)
O(2)	0.9219(5)	0.4993(4)	0.4427(3)	0.0078(12)	0.0065(26)	0.0060(27)	0.0104(27)	−0.0008(18)	0.0016(21)	−0.0013(18)
O(3)	0.6497(5)	0.3211(5)	0.4375(3)	0.0072(11)	0.0089(27)	0.0060(25)	0.0065(25)	−0.0002(19)	−0.0005(21)	−0.0001(19)
O(4)	0.8473(5)	0.3246(5)	0.5567(3)	0.0073(11)	0.0085(27)	0.0030(24)	0.0099(26)	−0.0017(19)	−0.0016(22)	−0.0024(19)
O(5)	0.1068(5)	0.1938(5)	0.5588(3)	0.0100(12)	0.0103(28)	0.0083(26)	0.0120(27)	0.0022(20)	0.0034(22)	0.0001(21)
O(6)	0.1820(5)	−0.0011(4)	0.4376(3)	0.0084(12)	0.0073(27)	0.0072(27)	0.0098(27)	0.0002(19)	−0.0043(21)	0.0004(19)
O(7)	0.6477(5)	0.6824(5)	0.4430(3)	0.0063(11)	0.0051(26)	0.0053(25)	0.0083(25)	−0.0025(19)	−0.0006(21)	−0.0008(19)
O(8)	0.8500(5)	0.6749(5)	0.5559(3)	0.0079(11)	0.0079(27)	0.0067(25)	0.0094(26)	0.0026(19)	0.0018(22)	−0.0016(19)
O(9)	−0.1058(5)	0.1949(5)	0.4421(3)	0.0100(12)	0.0092(28)	0.0085(26)	0.0131(27)	−0.0048(20)	0.0040(21)	−0.0012(21)
O(10)	0.6104(5)	0.8037(5)	0.5629(3)	0.0099(11)	0.0094(28)	0.0081(26)	0.0126(270	−0.0033(20)	0.0028(22)	−0.0038(21)
O(11)	0.3947(5)	−0.1945(5)	0.4453(3)	0.0097(11)	0.0096(27)	0.0059(25)	0.0140(27)	0.0037(20)	0.0037(22)	0.0014(20)
O(12)	0.3126(5)	0.0016(4)	0.5595(3)	0.0079(12)	0.0044(26)	0.0072(27)	0.0110(27)	−0.0005(19)	−0.0045(21)	−0.0010(18)
S	0.4887(2)	0.1094(2)	0.7406(1)	0.0107(5)	0.0115(10)	0.0112(9)	0.0094(10)	0.0002(7)	0.0011(7)	−0.0005(8)
O(13)	0.5242(5)	0.0252(5)	0.6717(3)	0.0186(13)	0.0295(32)	0.0138(27)	0.0132(28)	0.0033(21)	0.0056(24)	−0.0013(23)
O(14)	0.9158(6)	0.4892(6)	0.2890(3)	0.0297(15)	0.0403(38)	0.0351(35)	0.0150(31)	0.0004(24)	0.0089(27)	0.0223(27)
O(15)	0.6095(5)	0.1637(6)	0.7855(3)	0.0212(13)	0.0206(30)	0.0242(30)	0.0171(29)	0.0008(22)	−0.0067(23)	−0.0075(24)
O(16)	0.4075(5)	0.2392(6)	0.7142(3)	0.0241(13)	0.0248(31)	0.0211(30)	0.0257(30)	−0.0037(23)	−0.0003(24)	0.0144(24)
OW(1)	−0.1529(5)	−0.2224(6)	0.2225(3)	0.0245(13)	0.0223(32)	0.0228(30)	0.0293(33)	0.0024(25)	0.0066(25)	0.0011(25)

Table 5
continued

	x	y	z	U_{eq}*	U_{11}	U_{22}	U_{33}	U_{23}	U_{13}	U_{12}
H(1)	−0.246(2)	−0.208(7)	0.228(4)		0.0294					
H(2)	−0.124(6)	−0.318(5)	0.247(4)		0.0294					
OW(2)	0.7271(7)	0.4018(8)	0.6938(4)	0.0518(19)	0.0623(49)	0.0602(50)	0.0342(38)	−0.0060(35)	0.0110(34)	−0.0357(39)
H(3)	0.775(9)	0.490(7)	0.717(5)		0.0622					
H(4)	0.703(9)	0.334(8)	0.735(4)		0.0622					
OW(3)	−0.0255(7)	0.0065(6)	0.3135(3)	0.0339(16)	0.0446(41)	0.0292(36)	0.0265(35)	0.0051(25)	−0.0035(30)	−0.0056(28)
H(5)	−0.034(8)	0.088(5)	0.275(3)		0.0406					
H(6)	−0.061(8)	−0.087(4)	0.289(3)		0.0406					
H(7)	0.620(2)	0.484(7)	0.609(2)		0.0080					
H(8)	0.892(7)	0.497(7)	0.386(1)		0.0094					
H(9)	0.648(7)	0.317(7)	0.3797(8)		0.0087					
H(10)	0.844(7)	0.320(7)	0.6140(9)		0.0088					
H(11)	0.088(6)	0.118(6)	0.598(3)		0.0120					
H(12)	0.130(6)	0.003(7)	0.386(2)		0.0101					
H(13)	0.626(6)	0.697(7)	0.386(1)		0.0076					
H(14)	0.865(7)	0.678(7)	0.6139(8)		0.0095					
H(15)	−0.087(6)	0.118(6)	0.403(3)		0.0120					
H(16)	0.596(7)	0.874(6)	0.606(3)		0.0119					
H(17)	0.411(7)	−0.134(6)	0.399(2)		0.0116					
H(18)	0.371(6)	0.011(7)	0.609(2)		0.0094					

Table 6
Selected interatomic distances (Å) and angles (°) for nickelalumite

M−O(1)	2.093(5)	Al(1)−O(2)	1.933(5)	Al(2)−O(1)	1.935(5)	Al(3)−O(5)	1.894(5)
M−O(2)	2.045(5)	Al(1)−O(2)a	1.949(5)	Al(2)−O(1)b	1.964(5)	Al(3)−O(6)	1.859(5)
M−O(3)	2.065(5)	Al(1)−O(4)	1.906(5)	Al(2)−O(3)	1.913(5)	Al(3)−O(7)	1.972(5)
M−O(4)	2.104(5)	Al(1)−O(5)	1.839(5)	Al(2)−O(7)	1.922(5)	Al(3)−O(8)	1.948(5)
M−O(7)	2.062(5)	Al(1)−O(8)	1.903(5)	Al(2)−O(10)	1.837(5)	Al(3)−O(10)	1.884(5)
M−O(8)	2.107(5)	Al(1)−O(9)	1.847(5)	Al(2)−O(1)	1.831(5)	Al(3)−O(12)	1.851(5)
<M−O>	2.079	<Al(1)−O>	1.896	<Al(2)−O>	1.900	<Al(3)−O>	1.901
Al(4)−O(3)	2.006(5)	S−O(13)	1.470(5)	O(13)−S−O(14)	109.3(3)		
Al(4)−O(4)	1.966(5)	S−O(14)	1.460(5)	O(13)−S−O(15)	108.9(3)		
Al(4)−O(6)	1.867(5)	S−O(15)	1.474(5)	O(13)−S−O(16)	109.3(3)		
Al(4)−O(9)	1.877(5)	S−O(16)	1.468(5)	O(14)−S−O(15)	110.6(3)		
Al(4)−O(11)	1.858(5)	<S−O>	1.468	O(14)−S−O(16)	109.8(4)		
Al(4)−O(12)	1.842(5)			O(15)−S−O(16)	109.0(3)		
<Al(4)−O>	1.903			<O−S−O>	109.5		
a: x−1, y, z; b: −x + 1, −y + 1, −z + 1							

Table 7
Hydrogen bonding in the crystal structure of nickelalumite

D − H…A	D − A (Å)	D − H (Å)	H − A (Å)	∠D − H…A (°)
*W(1)−H(1)−O(16)	2.926(5)	0.98(1)	2.03(1)	151.4(6)
W(1)−H(1)−O(14)	3.277(4)	0.98(1)	2.67(1)	139.9(1)
W(1)−H(2)−O(14)	2.863(4)	0.98(1)	1.89(1)	174.5(5)
W(1)−H(2)−O(13)	3.406(4)	0.98(1)	2.80(1)	120.7(5)
W(2)−H(3)−O(15)	2.870(5)	0.99(3)	1.95(1)	154.1(4)
W(2)−H(3)−O(13)	3.442(5)	0.99(3)	2.68(1)	134.2(4)
W(2)−H(4)−O(15)	2.958(4)	0.97(2)	2.03(1)	158.9(4)
W(3)−H(5)−O(16)	2.869(5)	0.98(1)	1.91(1)	163.8(5)
W(3)−H(5)−O(15)	3.294(4)	0.98(1)	2.65(1)	123.5(1)
W(3)−H(6)−W(1)	2.805(4)	0.98(1)	1.86(1)	162.8(1)
∠H(1)−W(1)−H(2)	109.1(1.7)			
∠H(3)−W(2)−H(4)	110.7(3.0)			
∠H(5)−W(3)−H(6)	109.4(1.8)			
O(1)−H(7)−W(2)	2.822(5)	0.99(1)	1.88(1)	157.7(1)
O(2)−H(8)−O(14)	2.625(5)	0.99(1)	1.70(1)	153.6(1)
O(3)−H(9)−W(1)	2.765(4)	0.99(1)	1.79(1)	170.2(1)
O(4)−H(10)−W(2)	2.837(4)	0.99(1)	2.04(1)	137.1(1)
O(5)−H(11)−W(3)	2.998(5)	0.99(1)	2.02(1)	168.9(1)
O(6)−H(12)−W(3)	2.858(4)	0.99(1)	1.93(1)	156.6(1)
O(7)−H(13)−O(16)	2.782(4)	0.99(1)	1.81(1)	169.5(1)
O(8)−H(14)−O(15)	2.707(5)	0.99(1)	1.72(1)	174.0(1)
O(9)−H(15)−W(3)	2.944(5)	0.99(1)	1.98(1)	165.6(1)
O(10)−H(16)−O(13)	2.904(3)	0.99(1)	1.94(1)	164.1(1)
O(11)−H(17)−O(13)	2.698(4)	0.99(1)	1.73(1)	166.2(1)
O(12)−H(18)−O(13)	2.762(5)	0.99(1)	1.82(1)	157.4(1)
* W: oxygen atom of an (H$_2$O) group				

Table 8
Refined site-scattering values (*epfu*) and assigned site-populations (*apfu*) for nickelalumite

	Refined site-scattering	Site population	Calculated site-scattering	<X−φ>$_{calc.}$*	<X−φ>$_{obs.}$
M	27.63(15)	0.55Ni + 0.39Zn + 0.02V + 0.01e	27.82	2.089	2.079
* Calculated by summing constituent ionic radii; values from Shannon (1976)					

Description Of The Structure

Cation sites

There are five octahedrally coordinated sites in the nickelalumite structure. The *M* site is occupied by Ni and Zn with minor V and Fe: (Ni$_{0.55}$Zn$_{0.39}$V$_{0.02}$Fe$_{0.01}$)$_{\Sigma0.97}$, <*M*−OH > = 2.079 Å. There are four sites occupied solely by Al, with < *Al*−OH > = 1.900 Å. There is one tetrahedrally coordinated *S* site with < *S*−O > = 1.468 Å. There are twelve anion sites occupied by (OH) groups and three sites fully occupied by (H$_2$O). The refined and calculated site-scattering values and the observed and calculated < X−φ > distances (φ = unspecified ligand) are in accord with the site populations in Table 8.

Structure topology

In the nickelalumite structure, *Al* octahedra are connected through common edges to form six-membered rings with an octahedron at the centre of the ring. Half of these octahedra are occupied by Ni and Zn, and half are vacant. *M* and *Al* octahedra form a [(Ni,Zn)Al$_4$(OH)$_{12}$]$^{2+}$ sheet parallel to (001) (Fig. 8a). The

(SO_4) tetrahedra and (H_2O) groups occupy interstitial space between sheets of $M-Al$ octahedra (Fig. 9a), and (SO_4) tetrahedra link by hydrogen bonds involving donor O-atoms of (H_2O) groups and acceptor O-atoms of (SO_4) tetrahedra (Figs. 9a, 10a, Table 7). Hydrogen bonds link donor O-atoms of (OH)-groups to acceptor O-atoms of (H_2O) groups and (SO_4) tetrahedra (Figs. 9a, 10a) to link the [(Ni,Zn)Al$_4$(OH)$_{12}$] structural unit to the interstitial {(SO_4)(H_2O)$_3$} layer.

Relation To Other Structures

Nickelalumite has stoichiometry (Table 2) similar to that of kyrgyzstanite: (Zn, Ni)(Al$_4$(SO$_4$)(OH)$_{12}$(H$_2$O)$_3$, (Agakhanov et al., 2005), mbobomkulite:

(Ni, Cu^{2+})Al$_4$[(NO$_3$),(SO$_4$)]$_2$(OH)$_{12}$(H$_2$O)$_3$, hydrombobomkulite: (Ni,Cu^{2+})Al$_4$[(NO$_3$),(SO$_4$)]$_2$(OH)$_{12}$ (H$_2$O)$_{12}$ (Martini 1980) and chalcoalumite: CuAl$_4$(SO$_4$) (OH)$_{12}$(H$_2$O)$_3$ (Larsen and Vassar 1925; Williams and Khin 1971). The crystal structures of nickelalumite and kyrgyzstanite were solved by Uvarova et al. (2005) and Agakhanov et al. (2005), and the structure of chalcoalumite was eventually refined by Hawthorne and Cooper (2013) on a rotating-anode diffractometer. The similarity of the stoichiometries, cell dimensions and space groups of mbobomkulite and hydrombobomkulite (Table 9) suggest that the former is isostructural with chalcoalumite (the earliest named member of the group) and the latter has a related structure.

Table 9
Comparison of data for nickelalumite, kyrgyzstanite, mbobomkulite, hydrombobomkulite, chalcoalumite, alvanite and ankinovichite

Mineral name	Ideal formula	Space group	a, Å	b, Å	c, Å	$β$, º	Z	Ref.
Nickelalumite	NiAl$_4$(SO$_4$)O$_{12}$(H$_2$O)$_3$	$P2_1/n$	10.2567(5)	8.8815(4)	17.0989(8)	95.548(1)	4	(1)
Kyrgyzstanite	ZnAl$_4$(OH)$_{12}$(SO$_4$)(H$_2$O)$_3$	$P2_1/n$	10.246	8.873	17.220	96.41	4	(2)
Mbobomkulite	(Ni,Cu^{2+})Al$_4$[(NO$_3$),(SO$_4$)]$_2$ (OH)$_{12}$(H$_2$O)$_3$	undetermined	10.171	8.865	17.145	95.37	4	(3)
Hydrombobomkulite	(Ni,Cu^{2+})Al$_4$[(NO$_3$),(SO$_4$)]$_2$ (OH)$_{12}$(H$_2$O)$_{12}$	undetermined	10.145	17.155	20.870	90.55	4	(3)
Chalcoalumite	CuAl$_4$(SO$_4$)(OH)$_{12}$(H$_2$O)$_3$	$P2_1/n$	10.228(3)	8.929(3)	17.098(6)	95.800(11)	4	(4)
Alvanite	ZnAl$_4$(VO$_3$)$_2$(OH)$_{12}$(H$_2$O)$_2$	$P2_1/n$	17.808(8)	5.132(3)	8.881(4)	92.11(3)	2	(5)
Ankinovichite	NiAl$_4$(VO$_3$)$_2$(OH)$_{12}$(H$_2$O)$_2$	$P2_1/n$	17.8098(8)	5.1228(2)	8.8665(4)	92.141(1)	2	(6)
References: (1) Uvarova et al. (2005); (2) Agakhanov et al. (2005); (3) Martini (1980); (4) Hawthorne and Cooper (2013); (5) Pertlik and Dunn (1990); (6) Karpenko et al. (2004b)								

The crystal structure of nickelalumite involves a [NiAl$_4$(OH)$_{12}$] sheet (Fig. 8a) topologically identical to the analogous [ZnAl$_4$(OH)$_{12}$] sheet (Fig. 8b) in alvanite, ideally ZnAl$_4$(VO$_3$)$_2$(OH)$_{12}$(H$_2$O)$_2$ (Pertlik and Dunn 1990), and ankinovichite NiAl$_4$(VO$_3$)$_2$(OH)$_{12}$(H$_2$O)$_2$ (Karpenko et al. 2004b). In the structure of nickelalumite, [NiAl$_4$(OH)$_{12}$] sheets are connected through isolated (SO$_4$) tetrahedra and (H$_2$O) groups (Figs. 9a, 10a) whereas in alvanite and ankinovichite, layers of octahedra are linked by hydrogen bonds to unbranched [TO$_3$] chains (Figs. 9b, 10b), a very common linkage of tetrahedra in minerals (Day and Hawthorne 2020, 2022). The differences between the nickelalumite-type structure and the alvanite-type structure are best shown by their interstitial layers (Fig. 10). In the nickelalumite structure, sulfate tetrahedra are linked by hydrogen bonds involving interstitial (H$_2$O) groups (Figs. 9a, 10a), whereas in the alvanite structure, [VO$_3$] chains of tetrahedra link *via* hydrogen bonds involving chains of hydrogen-bonded (H$_2$O) groups (Figs. 9b, 10b). The different two-dimensional packing arrangements of these two interstitial layers accounts for the different content of (H$_2$O) in each structure type: (H$_2$O)$_3$ in nickelalumite (Fig. 10a) and (H$_2$O)$_2$ in alvanite (Fig. 10b).

Declarations

References

1. Agakhanov AA, Karpenko VY, Pautov LA, Uvarova YA, Sokolova E, Hawthorne FC, Bekenova GK (2005) Kyrgyzstanite, $ZnAl_4(SO_4)(OH)_{12}(H_2O)_3$ – a new mineral from the Kara–Tangi, Kyrgyzstan. New Data on Minerals 40:23–28

2. Bartelmehs KL, Bloss FD, Downs RT, Birch JB (1992) Excalibr II. Z Krystallogr 199:185–196

3. Day MC, Hawthorne FC (2020) A structure hierarchy for silicate minerals: Chain, ribbon, and tube silicates. Mineral Mag 84:165–244

4. Day MC, Hawthorne FC (2022) Bond topology of chain, ribbon and tube silicates. Part I. Graph- theory generation of infinite one-dimensional arrangements of $(TO_4)^{n-}$ tetrahedra. Acta Crystallogr A78:212–233

5. Hawthorne FC, Cooper MA (2013) The crystal structure of chalcoalumite: mechanisms of Jahn-Teller-driven distortions in $^{[6]}Cu^{2+}$-containing oxysalts. Mineral Mag 77:2901–2912

6. Karpenko VV, Agakhanov AA, Pautov LA, Dikaya TV, Bekenova GK (2004a) New occurrence of nickelalumite on Kara–Chagyr, South Kirgizia. New Data on Minerals 39:32–39

7. Karpenko VV, Agakhanov AA, Pautov LA, Sokolova E, Hawthorne FC, Agakhanov AA, Dikaya TV, Bekenova GK (2004b) Ankinovichite, nickel analogue of alvanite, a new mineral from Kurunsak (Kazakhstan) and Kara-Chagyr (Kirgizia). Zap Vser Mineral Obshchest 133(2):59–70 (in Russian)

8. Karpenko VYu, Pautov LA, Agakhanov AA (2009) Discovery of low aluminium nevadaite from the Kara Chagyr area, Kyrgyzstan. Geology of Ore Deposits 51:794–799

9. Karpenko VYu, Pautov LA, Agakhanov AA, Bekenova GK (2011) On mannardite from vanadium-bearing schists of Kazakhstan and Central Asia. New Data on Minerals 46:25–33

10. Karpenko VYu, Pautov LA, Agakhanov AA (2016) About Ni-Zn-bearing volborthite ("uzbekite") from vanadium-bearing schists of Southern Kyrgyzstan. New Data on Minerals 51:20–29

11. Larsen ES, Vassar HE (1925) Chalcoalumite, a new mineral from Bisbee, Arizona. Am Mineral 10:79–83

12. Martini JEJ (1980) Mbobomkulite, hydrombobomkulite, and nickelalumite, new minerals from Mbobo Mkulu cave, eastern Transvaal. Ann Geol Surv S Afr 14:1–110 (reference obtained from Am Mineral 67:415–416, 1982)

13. Merlet C (1992) Quantitative electron probe microanalysis: new accurate $\Phi(\rho z)$ description. Mikrochim Acta 12:107–115

14. Pertlik F, Dunn PJ (1990) Crystal structure of alvanite, $(Zn,Ni)Al_4(VO_3)_2(OH)_{12} \cdot 2H_2O$, the first example of an unbranched zweier-single chain vanadate in nature. Neues Jb Mineral Monat 385–392

15. Porshnyakov GS, Kotov NV, Kol'tsov AB, Vaganov PA, Zakharevich KV, Zubtsov SYe, Donskikh AV, Nesterov AR, Poritskaya LG (1991) Geological position and petrological and geochemical features of gold ore metasomatites in black shale strata. Vladivostok: DVO AN SSSR. 47 p. (in Russian)

16. Preobrazhensky IA (1926) Deposits of radioactive minerals in Western Fergana. Proceedings on the study of radium and radioactive ores: II, 73–120 (in Russian)

17. Scherbakov DI (1924) Deposits of radioactive ores and minerals of the Fergana and tasks for their further investigation. In: Materials for studying the natural productive forces of Russia. 47: 1–9 (in Russian)

18. Shannon RD (1976) Revised effective ionic radii and systematic studies of interatomic distances in halides and chalcogenides. Acta Crystallogr A32:751–767

19. Sheldrick, G.M. (2008) A short history of SHELX. Acta Crystallogr A64:112–122

20. Uvarova YA, Sokolova E, Hawthorne FC, Karpenko V, Agakhanov AA, Pautov LA (2005) The crystal chemistry of the "nickelalumite"-group minerals. Can Mineral 43:1511–1519

21. Williams GR, Moorehouse SJ, Prior TJ, Fogg AM, Rees NH, O'Hare D (2011) New insights into the intercalation chemistry of $Al(OH)_3$. Dalton Trans 40:6012–6022

22. Williams SA, Khin BS (1971) Chalcoalumite from Bisbee, Arizona. Mineral Rec 2:126–127
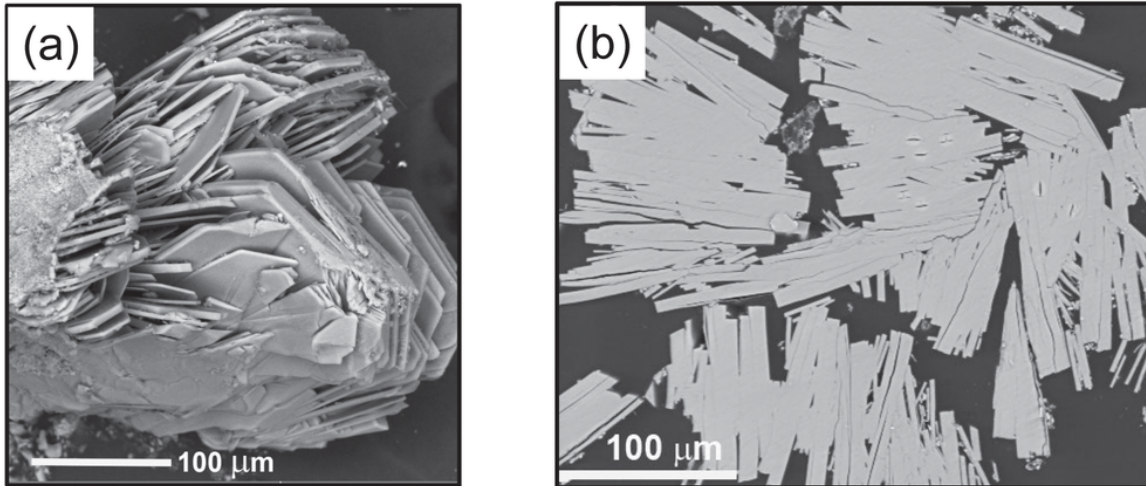
Figures
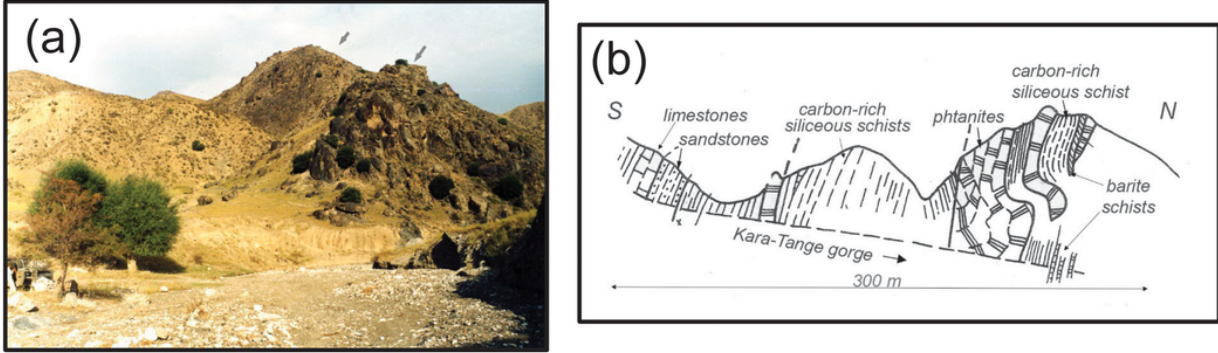
Figure 1

The Kara-Tangi deposit: (a) a view of the deposit; the locations of the blocks of black schist mined for uranium are indicated by black arrows; (b) sketch of the geology across the Kara-Tangi valley (from Porshnyakov et al. 1991)
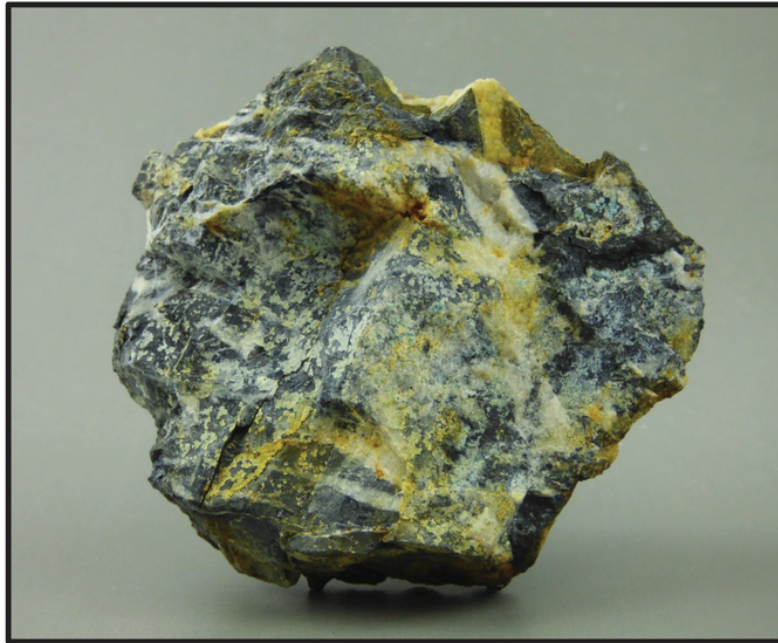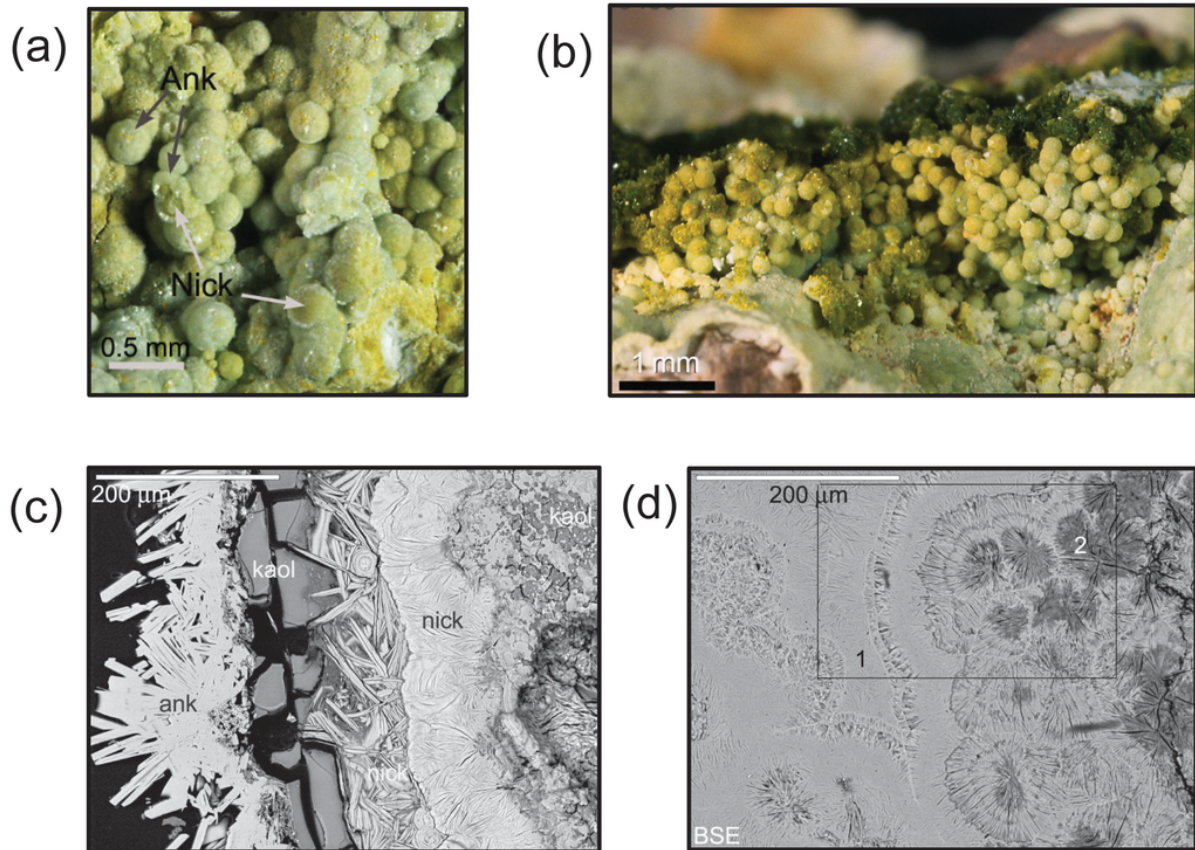
Figure 2

A typical hand-specimen (6.0 x 7.5 cm) of carbon-rich U−V-bearing black schist (black), penetrated by quartz veins and covered with greenish-bluish crystalline crust mainly of nickelalumite and kyrgyzstanite, Kara-Tangi dumps

Figure 3

An aggregation of lamellar split crystals of nickelalumite from Kara-Tangi: (a) three-dimensional image; (b) polished section in BSE mode. Photo by I.B. Afanasyev

Figure 4

Spherulite aggregations of nickelalumite from Kara-Chagyr: (a) ankinovichite (Ank) overgrowth on nickelalumite (Nick); (b) spherulites of V-bearing nickelalumite with volborthite (Volb); (c) BSE image of cross-cut ankinovichite (ank) − nickelalumite (nick) crust witThe Raman spectrum of nickelalumite: (a) Kara-Tangi, Kyrgyzstan; (b) Mbobo Mkulu, R.S.A.h kaolinite (kaol); (d) BSE image of cross-cut of nickelalumite (1) and Si-V-rich nickelalumite (2) as part of the complex zoned spherulite; frame shows area covered by image (c). Photos (a) and (b) by N.A. Pekova
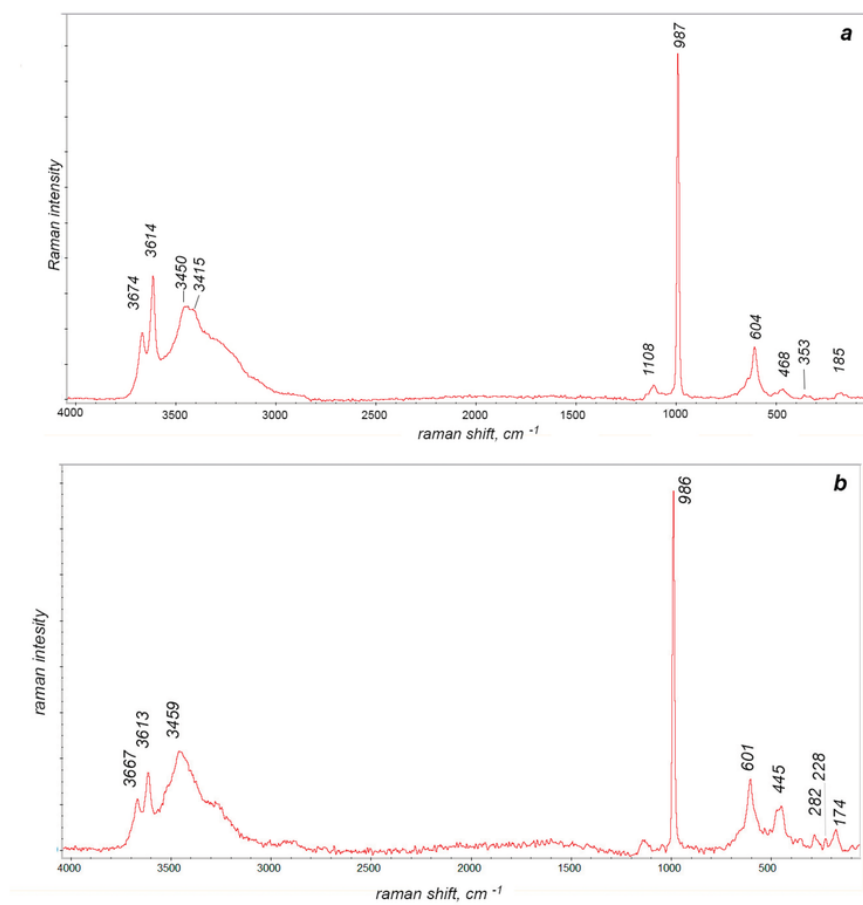
Figure 5

The Raman spectrum of nickelalumite: (a) Kara-Tangi, Kyrgyzstan; (b) Mbobo Mkulu, R.S.A.
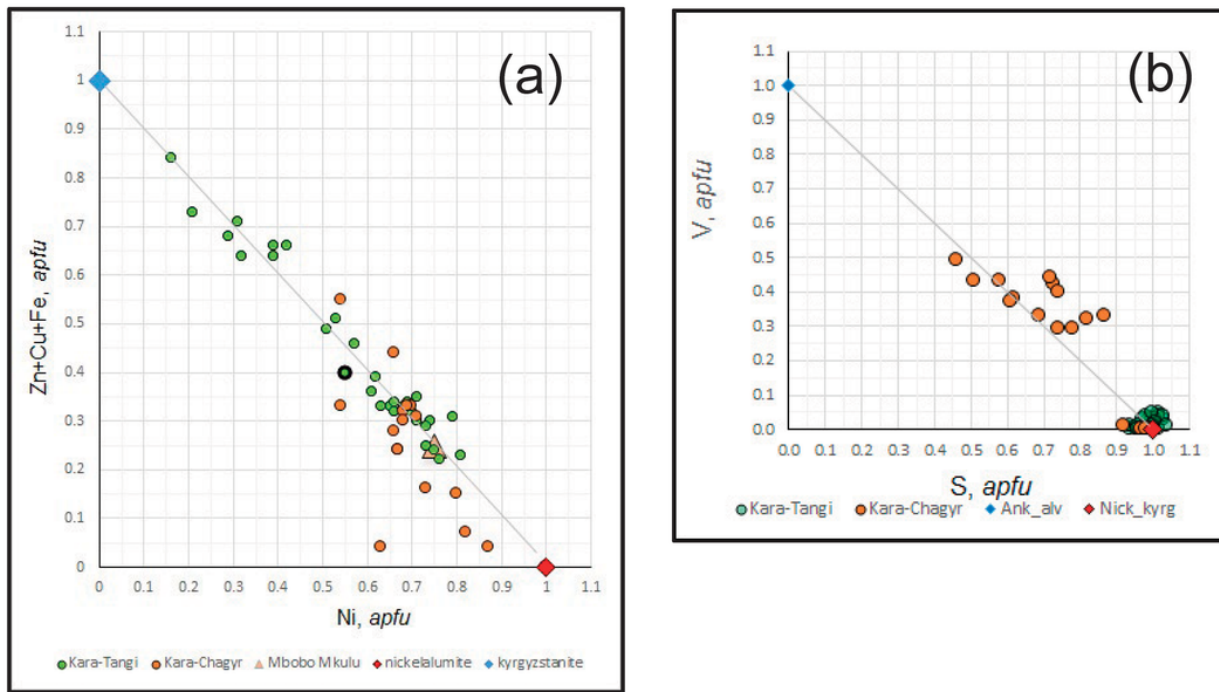
Figure 6

Compositional variation in nickelalumite from Kara-Chagyr (red circles) and Kara-Tangi (green circles); (a) (Zn + Cu + Fe) *vs*. Ni; (b) V *vs*. S
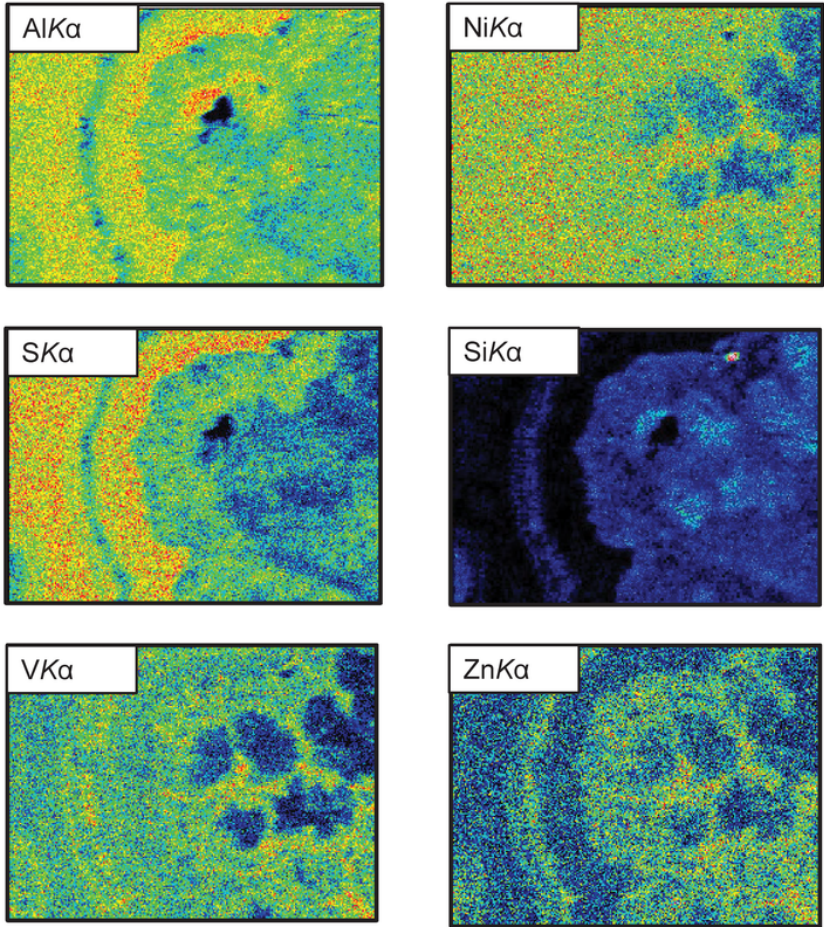
Figure 7
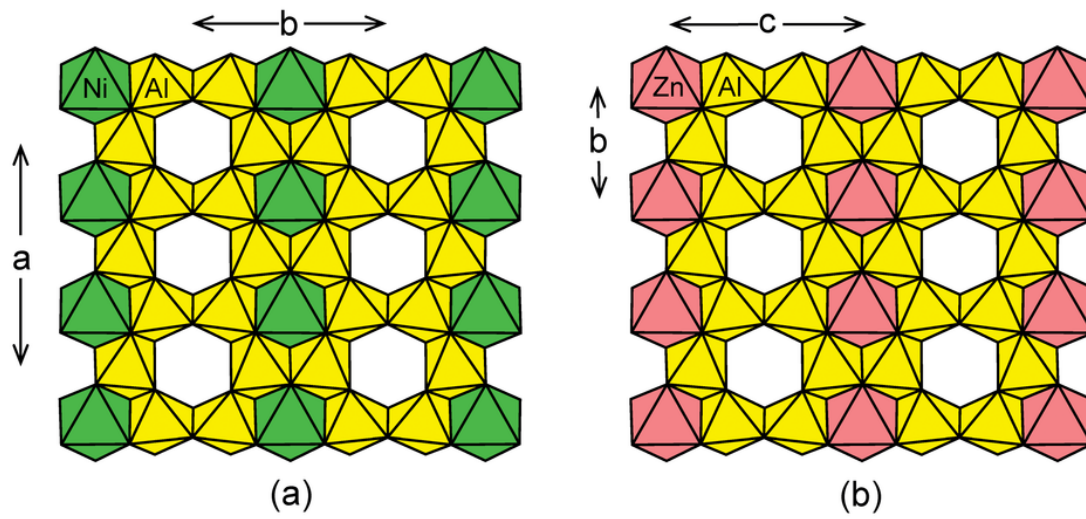
X-ray maps of the area in the frame on Fig. 4d

Figure 8

(a) The $[NiAl_4(OH)_{12}]$ sheet in nickelalumite and (b) the analogous $[ZnAl_4(OH)_{12}]$ sheet in alvanite. Ni octahedra: green; Al octahedra: yellow; Zn octahedra: orange
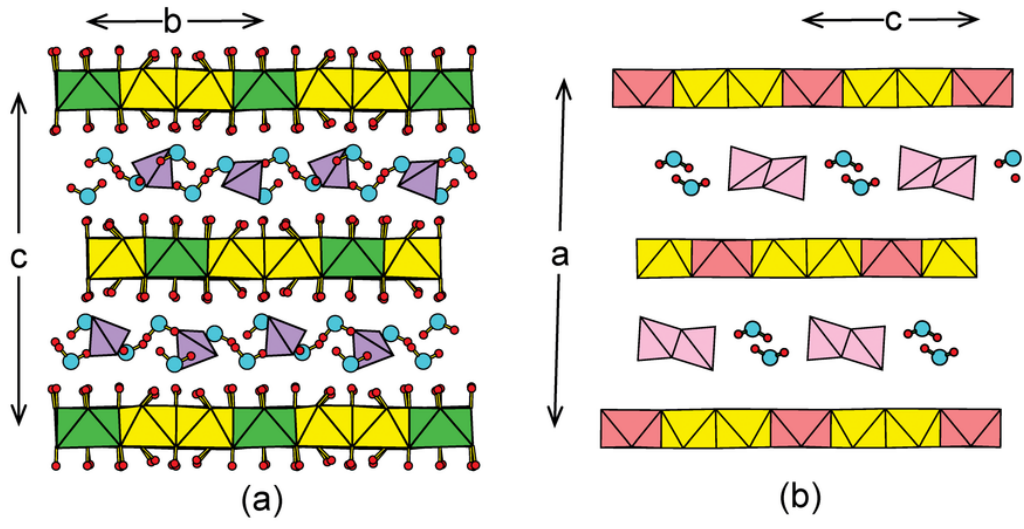
Figure 9

Interleaved sheets of $[M^{2+}Al_4(OH)_{12}]$ and layers of $\{(TO_4)_n(H_2O)_m\}$ in (a) nickelalumite and (b) alvanite. Legend as in Fig. 8; (SO_4) groups: mauve; (VO_4) groups: pink; O atoms: pale-blue circles; H atoms: small red circles
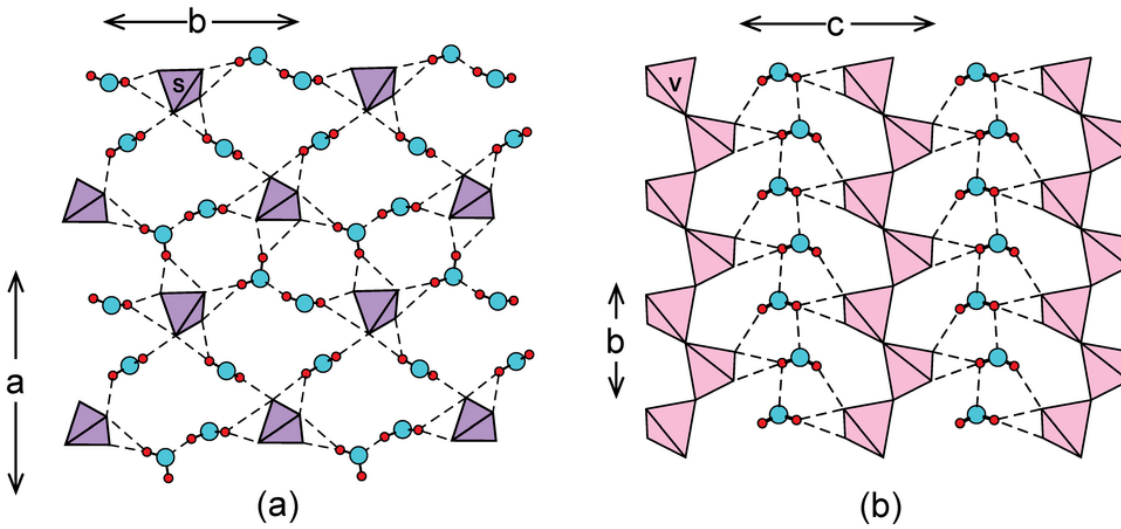
Figure 10

The interstitial layers in (a) nickelalumite and (b) alvanite. Legend as in Fig. 9; O_W–H bonds are shown as solid black lines and hydrogen bonds are shown as dashed black lines

Supplementary Files

This is a list of supplementary files associated with this preprint. Click to download.

- Nickelalumitecif.cif